Atmos. Chem. Phys. Discuss., 13, 9917–9952, 2013
www.atmos-chem-phys-discuss.net/13/9917/2013/
doi:10.5194/acpd-13-9917-2013
© Author(s) 2013. CC Attribution 3.0 License.

Atmospheric Chemistry and Physics
Open Access
Discussions

This discussion paper is/has been under review for the journal Atmospheric Chemistry and Physics (ACP). Please refer to the corresponding final paper in ACP if available.

Aerosol loading in the Southeastern United States: reconciling surface and satellite observations

B. Ford[1] **and C. L. Heald**[2]

[1]Department of Atmospheric Science, Colorado State University, Fort Collins, CO, USA
[2]Department of Civil and Environmental Engineering and Department of Earth, Atmospheric and Planetary Sciences, MIT, Cambridge, MA, USA

Received: 25 February 2013 – Accepted: 11 March 2013 – Published: 15 April 2013

Correspondence to: B. Ford (bonne@atmos.colostate.edu)

Published by Copernicus Publications on behalf of the European Geosciences Union.

Abstract

We investigate the seasonality in aerosols over the Southeastern United States using observations from several satellite instruments (MODIS, MISR, CALIOP) and surface network sites (IMPROVE, SEARCH, AERONET). We find that the strong summertime enhancement in satellite-observed aerosol optical depth (factor 2–3 enhancement over wintertime AOD) is not present in surface mass concentrations (25–55 % summertime enhancement). Goldstein et al. (2009) previously attributed this seasonality in AOD to biogenic organic aerosol; however, surface observations show that organic aerosol only accounts for ∼35 % of $PM_{2.5}$ mass and exhibits similar seasonality to total $PM_{2.5}$. The GEOS-Chem model generally reproduces these surface aerosol measurements, but under represents the AOD seasonality observed by satellites. We show that seasonal differences in water uptake cannot sufficiently explain the magnitude of AOD increase. As CALIOP profiles indicate the presence of additional aerosol in the lower troposphere (below 700 hPa), which cannot be explained by vertical mixing; we conclude that the discrepancy is due to a missing source of aerosols above the surface in summer.

1 Introduction

Portmann et al. (2009) suggest that increases in atmospheric aerosols of biogenic origin associated with regional reforestation may have caused cooling over the Southeastern United States (SEUS) in recent decades. This theory is supported by the strong winter to summer seasonality in satellite-derived aerosol optical depth (AOD) that spatially and temporally matches biogenic volatile organic compound (BVOC) emissions in the region (Goldstein et al., 2009). A potential source of this summertime aerosol could be enhanced production of secondary organic aerosols (SOA) formed from the oxidation of volatile organic compounds (VOC) emitted from vegetation in the presence of anthropogenic pollutants from urban areas (Volkamer et al., 2006; Hoyle et al., 2011).

cc BY

The SEUS could be particularly susceptible to such an effect (Weber et al., 2007), which could augment summertime aerosol loading in the region.

The SEUS is densely forested and mostly a rural environment although there are also several major urban centers in the region. Previous studies have shown that $PM_{2.5}$ concentrations in the region are dominated by ammonium sulfate and organic matter (OM), which together account for 60–90 % of the surface $PM_{2.5}$ concentrations (Edgerton et al., 2005; Weber et al., 2007; Hand et al., 2012; Zhang et al., 2012). Throughout most of the year, organic carbon is produced from wood combustion and diesel exhaust; secondary production dominates in the summertime (Zheng et al., 2002). Lim and Turpin (2002) suggest that SOA generally makes up half of the measured organic carbon. Although urban centers often have higher $PM_{2.5}$ concentrations and their emissions can have a regional impact, water soluble organic carbon concentrations, which are often used as a marker for SOA, appear to have a more homogenous source over the region (Peltier et al., 2007).

Several studies have also suggested that aerosol loading over the Southeastern US has decreased over the last decade. Edgerton et al. (2005) note a 15–20 % decrease in surface $PM_{2.5}$ mass in the region over the five-year period from 1999–2003, mainly attributable to declines in sulfate and organic matter. Using satellite measurements of AOD and surface $PM_{2.5}$ measurements over Georgia, Alston et al. (2012) also suggest that aerosol loading over the Southeastern US declined from 2000–2009. Additionally, Leibensperger et al. (2012) suggest that anthropogenic aerosols are responsible for regional cooling over the Eastern US over the last century, but that this radiative forcing has declined since 1990 mainly due to decreases in domestic emissions of sulfur dioxide. However, given limitations in both our measurement and understanding of BVOC emissions and SOA formation (Hallquist et al., 2009), it is unclear whether biogenic emissions, and the aerosols produced upon oxidation of these emissions, have also changed over this same time period. The evolution of these biogenic emissions is difficult to predict (e.g. Heald et al., 2009), representing a significant hurdle for future air quality management efforts and the prediction of climate forcing.

cc BY

In this study, we use a suite of satellite and surface observations with a global model to explore the origin of the observed enhancement of summertime AOD in the SEUS. We aim to provide insight relevant to the Southern Oxidant and Aerosol Study (SOAS) campaign in 2013, whose primary objective is to investigate the impact of biogenic aerosol on regional climate and air quality.

2 Description of observations and model

2.1 Satellite observations

For this study, we use a variety of satellite instruments and products to analyze aerosol and cloud distributions and variability along with fire activity.

The Multi-imaging Spectroradiometer (MISR) instrument was launched into sun-synchronous orbit aboard the EOS-Terra satellite in 1999 and provides global measurements of AOD with an equator crossing of ∼10:30 a.m. local time. MISR employs nine different cameras to make multi-angle radiance measurements in four spectral bands (visible to near infrared). Here we use the Level 3 daily averaged AOD at 555 nm gridded and filtered to remove any pixels containing Level 2 AOD data with a standard deviation of greater than 2.5.

The Moderate Resolution Imaging Spectroradiometer (MODIS) measures radiances at 36 wavelengths to characterize a variety of land and atmospheric properties. We use observations here from the MODIS instrument launched aboard the EOS-Aqua platform in 2002, which flies as part of the A-Train constellation, making simultaneous measurements at an equator crossing of 13:30 local time. AOD from MODIS is retrieved separately over the ocean and land to account for differences in surface properties. While some studies have found a high AOD bias in the western US due to the use of an estimated surface reflectance over the bright land surface (Drury et al., 2010), the SEUS has dense vegetation that provides good dark targets and greater confidence in the MODIS aerosol retrieval (Roy et al., 2007). For this work, we use Collection 5,

cc BY

Level 3 daily measurements and combine land and ocean optical depth retrievals. We filter the MODIS data to include only grid boxes with cloud fractions below 0.5 and aerosol optical depths less that 1.5 following Zhang and Reid (2006). We note that the magnitude of AOD observed by MODIS is sensitive to the cloud fraction filtering (Zhang et al., 2006); however the spatial distribution and relative increase from winter to summer remain the same when cloud fraction filtering is varied from 0.1 to 0.8. To investigate the impact of biomass burning on aerosol loading, we also examined MODIS fire counts. For this, we use V005 MODIS Aqua $1^\circ \times 1^\circ$ monthly gridded active fire counts, which have frequently been used as an estimate of biomass burning activity (Duncan et al., 2003; Zeng et al., 2008; Zhang et al., 2010).

The Cloud-Aerosol Lidar with Orthogonal Polarization (CALIOP) measures the vertical profile of aerosol extinction. CALIOP was launched aboard the CALIPSO satellite in 2006 as part of the A-Train constellation. The instrument detects the intensity and orthogonally polarized components of backscattered radiation at two wavelengths, 532 nm and 1064 nm (Winker et al., 2003). Details of the data processing algorithms are given by Winker et al. (2009) and of the aerosol classification schemes by Omar et al. (2009). To filter CALIOP observations, we use cloud aerosol distinction (CAD) scores, extinction uncertainty values, atmospheric volume descriptors, extinction quality control (QC) flags and total column optical depths. We make the approximation that all extinction observations with a corresponding atmospheric volume descriptor that indicates clear air have zero aerosol extinction. For comparisons of simulated extinction profiles with observed profiles, we match clear sky CALIOP profiles with the corresponding grid box and apply a simple detection limit to the model profile following Ford and Heald (2012). For further information on the impact of our filtering and sampling methods, we refer the reader to Ford and Heald (2012). Although the nighttime data has a greater signal-to-noise ratio (SNR) due to the lack of noise from background solar illumination (Hunt et al., 2009); in Figure 1, we use daytime observations to coincide with the MODIS observations. Previous comparisons of seasonally averaged AOD from CALIOP show that daytime observations have only a slight low bias compared to

CC BY

the night observations in source and outflow regions, and a slight high bias over remote marine regions (Ford and Heald, 2012).

We re-grid the satellite AOD observations to a $2^\circ \times 2.5^\circ$ resolution and calculate daily averages. In order to preserve the amount of data, we do not co-sample all the data. However, co-sampling the data does not change the spatial distributions or the magnitude of seasonality reported in Sect. 3.

For seasonal cloud fraction over the SEUS, we compare observations from MODIS Aqua and MODIS Terra with observations from the CloudSat Cloud Profiling Radar. In particular, we use the CloudSat Level 2 Radar-Lidar GEOPROF Product for profiles of cloud fraction and the Cloudsat Auxiliary Data to convert above ground altitude to pressure coordinates for December 2008–2009. The GEOPROF product combines observations from both CALIOP, which is useful for observing thin cirrus clouds but is completely attenuated in deep clouds (optical depths >3), and the CloudSat Cloud Profiling Radar, which has a millimeter wavelength and is able to penetrate through most non-precipitating clouds (Stephens et al., 2002; 2008). To compare with two-dimensional spatial distributions of cloud fractions observed by MODIS, we use the maximum cloud fraction from each profile observed by CloudSat/CALIOP.

2.2 Ground-based data

We use observations from the global AERosol Robotic NETwork (AEORONET) of sun photometers in the SEUS (Holben et al., 1998). AERONET sites record AOD and aerosol properties at several wavelengths in the visible and near IR, and have been used for validation studies of satellite measurements (e.g. Remer et al., 2002). For this work, we use hourly Version 2, Level 2 measurements from the Walker Branch and UA Huntsville sites for months in 2008–2009.

We also use surface measurements of $PM_{2.5}$ concentrations from both the Interagency Monitoring of Protected Visual Environments (IMPROVE) and Southeastern Aerosol Research and Characterization (SEARCH) networks. Surface measurements of atmospheric composition from the IMPROVE network are taken over a 24-h period once in three days and are analyzed for the concentration of fine, total, and speciated particle mass (Malm et al., 1994). Ammonium mass is determined by assuming that sulfate and nitrate are fully neutralized, which means that this is an upper bound for the dry mass of ammonium. The IMPROVE network $PM_{2.5}$ values used in this study are the reconstructed fine mass (RCFM) determined by adding the values of ammonium sulfate, ammonium nitrate, soil, sea salt, elemental carbon and organic matter. We use 1.8 as the organic carbon to organic matter multiplier following Hand et al. (2012); though we note that this could be too high or too low at specific sites as Malm and Hand (2007) have given a range of 1.2 to 2.6.

The SEARCH network is composed of eight sites consisting of pairs of urban and rural/suburban locations in four states (AL, FL, GA, MS) which all measure meteorological parameters, gas phase pollutants and major $PM_{2.5}$ components (organic carbon, elemental carbon, sulfate, nitrate, ammonium, and trace metals) (Hansen et al., 2003; Edgerton et al., 2005, 2006). These sites have both continuous and 24-h integrated filter-based measurements of $PM_{2.5}$, and the sample frequency is every 3 days, except for at the sites located in Atlanta and Birmingham which report daily. However, we sample the data from these two sites to the same measurement days as the other sites.

SEARCH network $PM_{2.5}$ concentrations are calculated as the sum of sulfate, nitrate, ammonium, organic matter (using 1.8[OC]), elemental carbon, and major metal oxides (MMO). MMO is the sum of aluminum, calcium, iron, potassium, silica, and titanium in the highest oxidation state and is almost equivalent to the soil concentrations reported by the IMPROVE network. However, the soil equation used for the IMPROVE network makes corrections to account for a lower oxidation state of iron, contributions from other elements, and potassium from non-soil sources; so that $[\mathrm{SOIL}] = (2.20[\mathrm{Al}] + 2.49[\mathrm{Si}] + 1.63[\mathrm{Ca}] + 2.42[\mathrm{Fe}] + 1.94[\mathrm{Ti}])$ (Malm et al., 1994). We also note that this standard calculation of $PM_{2.5}$ for SEARCH sites does not include sea salt as included with the IMPROVE data (calculated as 1.8[Cl]), and chlorine has only been reported since 2009. To estimate species contributions to the total $PM_{2.5}$

Title Page
Abstract | Introduction
Conclusions | References
Tables | Figures
◀| |▶
◀ ▶
Back | Close
Full Screen / Esc
Printer-friendly Version
Interactive Discussion

cc BY

from the SEARCH sites, we use the assumptions for the IMPROVE measurements to include a modified soil concentration and a value for sea salt using chlorine measurements from 2009. We also use hourly TEOM measurements of total $PM_{2.5}$ mass concentrations to characterize the diurnal variation.

All eight of the SEARCH sites and several IMPROVE sites are co-located with nephelometers, which provide measurements of ambient relative humidity (RH). For comparisons of vertical profiles of RH, we also use ground based soundings from 8 NOAA sites (http://weather.uwyo.edu/upperair/sounding.html). Locations of these IMPROVE, SEARCH, and NOAA sounding sites are shown in Figs. 1 and 4.

2.3 GEOS-Chem

We use v9.01.01 of the GEOS-Chem chemical transport model, driven by GEOS-5 meteorology, in the nested grid configuration over North America ($0.5^\circ \times 0.667^\circ$ horizontal resolution). The GEOS-Chem aerosol simulation includes sulfate, nitrate, ammonium (Park et al., 2004), primary carbonaceous aerosols (Park et al., 2003), dust (Fairlie et al., 2007; Ridley et al., 2012), sea salt (Alexander et al., 2005), and secondary organic aerosols (SOA) (Henze et al., 2008). Aerosols and gases are removed by both wet and dry deposition in the model. The wet deposition scheme includes scavenging in convective updrafts, rainout and washout (Liu et al., 2001), while dry deposition of gases and aerosols is dependent on surface characteristics and meteorological conditions (Wesely, 1989; Wang et al., 1998). The EPA NEI99 inventory is used for most anthropogenic and biofuel emissions over the USA (Hudman et al., 2007; 2008); however, anthropogenic emissions of black and organic carbon follow Cooke et al. (1999) with the seasonality from Park et al. (2003). Biogenic VOC emissions are calculated interactively following MEGAN (Guenther et al., 2006), while year-specific biomass burning is specified according to the GFED2 inventory (van der Werf et al., 2006). We implement a fix for artificially low nighttime boundary layer heights in the GEOS-5 product as well as a 25 % reduction in the HNO_3 concentrations, both of which improve comparisons with surface nitrate observations in the United States as described by Heald et al. (2012).

We calculate surface $PM_{2.5}$ in the model by combining sulfate, nitrate, ammonium, elemental carbon, organic matter (organic carbon scaled by a factor of 1.8 to account for total organic matter, consistent with IMPROVE and SEARCH measurements), fine dust, and accumulation mode sea salt concentrations in the lowest grid box. For comparison with IMPROVE and SEARCH daily $PM_{2.5}$ measurements, we compute 24 h averages and sample the data to site locations and measurement days.

Aerosol optical depth in the model is calculated for a specific wavelength using the extinction efficiency (Q_{ext}), the column mass loading (M), effective radius (r_{eff}), and particle mass density (ρ), such that the AOD (τ) is calculated by the following equation (Tegen and Lacis, 1996):

$$\tau = \frac{3Q_{\text{ext}}M}{4r_{\text{eff}}\rho}\alpha M \tag{1}$$

The aerosol mass extinction efficiency is calculated with Mie code based on wavelength-resolved optical and size parameters for various aerosol types from the Global Aerosol Data Set (GADS) (Koepke et al., 1997), with recent updates based on (Drury et al., 2010; Jaegle et al., 2010; Ridley et al., 2012) at 7 relative humidity values (0, 50 %, 70 %, 80 %, 90 %, 95 %, 99 %). The extinction efficiency (α) for each grid box is calculated from local relative humidity conditions (Martin et al., 2003). In order to determine whether the observed seasonality in AOD can be attributed to changes in mass loading or mass extinction efficiency, we explored the sensitivity of the mass extinction efficiency to the observed seasonal changes in relative humidity (Sect. 3.2). For this purpose we used the properties of sulfate aerosol (Table 1), which exhibits the strongest relationship with relative humidity (i.e. the largest hygroscopicity).

3 Results

3.1 Seasonality in AOD and surface concentrations

We mimic the seasonal AOD comparisons of Goldstein et al. (2009) in Fig. 1 for 2007–2009 using observations from MODIS Aqua, MISR, and CALIOP. Figure 1 also shows the seasonal mean AOD measured by ground-based sun photometers at two AERONET sites in the SEUS.

Figure 1 shows that observed summertime AOD is consistently a factor of 2–3 higher than wintertime values in the SEUS. This is consistent with Alston et al. (2012) who find a threefold increase in summertime AOD over wintertime, although they use a finer resolution product and therefore show greater spatial variability. The magnitude of both the seasonal mean and the relative enhancement differs among instruments as shown in the figure, but is spatially consistent. Similar summertime enhancements are reported at AERONET sites in 2008–2009. Furthermore, the mix of afternoon (MODIS, CALIOP) and morning (MISR) overpass times, as well as the 24-h sampling at AERONET sites, suggests that this enhancement is evident throughout the day. Four independent observations, made with four different measurement techniques all indicate a large regional enhancement in summertime AOD.

We contrast these observations with the GEOS-Chem chemical transport model simulation. Simulated summertime enhancements in AOD through the Eastern US range from 15 to 40 %. While the model does show a summertime maximum in AOD over the Ohio River Valley and northeastern US associated with increases in sulfate via SO_2 oxidation (Chin et al., 2000) and stagnation events, it does not reproduce the strong observed seasonality in column AOD over the SEUS.

The fourth column of Fig. 1 shows the GEOS-Chem simulated surface concentrations of $PM_{2.5}$ overlaid with observations from the SEARCH and IMPROVE networks. Comparison with surface observations indicates that GEOS-Chem captures the spatial, seasonal, and diurnal (Fig. 2) variation of $PM_{2.5}$ in the Eastern US , consistent with previous studies (e.g. Heald et al., 2012; Leibensperger et al., 2012). However, Fig. 1

shows that the measured surface concentrations exhibit only a fraction of the seasonality in the column AOD observed by the satellite instruments, suggesting that changes in surface concentrations do not dictate the seasonality observed in AOD. This is in agreement with Alston et al. (2012), who show that the summertime enhancement in surface $PM_{2.5}$ in Georgia is considerably less than the AOD enhancement over the region. This presents an intriguing disconnect between surface and column measurements of aerosol loading in the SEUS.

In Fig. 3, we explore the chemical composition of surface $PM_{2.5}$ over the SEUS in winter and in summer. Overall, the model captures the chemical speciation and the seasonality of IMPROVE surface concentrations in the region (Fig. 3a), but somewhat underestimates the observed summertime enhancement (~55 % in the mean). The observed surface seasonality is mainly due to inorganic species. Both observed and simulated nitrate concentrations are higher in the wintertime, consistent with more favorable formation of ammonium nitrate at cooler temperatures, while the increase in observed summertime sulfate is the result of enhanced SO_2 oxidation (Chin et al., 2000). The model simulation underestimates the doubling in sulfate concentrations from winter to summer seen at IMPROVE sites (specifically the Appalachian sites), but does captures the summertime enhancement associated with dust transport from North Africa (Ridley et al., 2012).

Observed OM at IMPROVE sites in the SEUS is consistently ~2–4 $\mu g\,m^{-3}$, making up less than 35 % of mean observed $PM_{2.5}$, consistent with the analysis of Hand et al. (2012). Zhang et al. (2012a) find slightly higher OM/$PM_{2.5}$ fractions (40–50 %) in urban areas in the SEUS; however, when biomass burning events are removed, the fraction of water soluble OM/$PM_{2.5}$ that they observe is reduced to ~25 %. GEOS-Chem under predicts OM concentrations by about a factor of two, consistent with other regions of the world (Heald et al., 2011). However, the magnitude of OM seasonality is similar between the observations and model with very little variation in OM throughout the year (a 35 % increase in summer over winter), in agreement with values reported by Zhang et al. (2012a). We also compare these OM concentrations and seasonality with IMPROVE sites in the Northeastern US, where there is not as large of an increase in summertime AOD, and find similar values at the surface.

Observations from the SEARCH network show even less seasonal variability in $PM_{2.5}$ than the IMPROVE sites, as shown in Figure 3b, which also highlights the differences between rural and urban sites. As expected, $PM_{2.5}$ concentrations are greater at urban sites and in particular, sulfate and elemental carbon are higher. Additionally, although GEOS-Chem is able to simulate dust concentrations and seasonality at IMPROVE sites, it overpredicts summertime dust at SEARCH sites, especially rural sites. There are also slightly higher concentrations and more seasonality in the OM at urban sites, consistent with Yan et al. (2009). Overall, the OM fraction at these SEARCH sites is greater than observed at the IMPROVE sites (Fig. 3a). Thus the model underestimate of OM is also greater. However, even more so than the IMPROVE comparisons, both the SEARCH observations and the simulation of concentrations at these sites, show very little seasonal variation in the OM at both rural and urban sites. Additionally, there is little diurnal variability in $PM_{2.5}$ (Fig. 2), which confirms that the seasonality in surface concentrations is consistent throughout the day and that the comparison with satellite observations provided at two snapshots is not biased by the satellite overpass time.

We conclude that the seasonality in satellite AOD over the SEUS does not match the surface concentrations, or more specifically, organic aerosol at the surface. This contrasts other regions where previous studies have found good correlation between satellite-observed column AOD and surface concentrations (e.g. Engel-Cox et al., 2004; Al-Saadi et al., 2005; van Donkelaar et al., 2006; Zhang et al., 2009; van Donkelaar et al., 2010). These previous studies note that discrepancies often arise in comparing surface concentrations and column AOD due to inaccurate assumptions or lack of information about the hygroscopicity of the aerosols, the composition, size distributions, the vertical distribution of aerosols, the presence of transported aerosols above the surface, and the meteorological environment, especially with regards to clouds. Correlations are highest when the aerosol is near the surface, uniformly mixed, relative

cc BY

humidity is moderate, and coarse mode aerosol fraction is small (Al-Saadi et al., 2005; van Donkelaar et al., 2006). Therefore, in the following sections we investigate several of these factors in an attempt to determine what, other than surface concentrations, could be driving the seasonality in AOD

3.2 Effect of relative humidity

Changes in aerosol water uptake could play a role in the seasonality of AOD in the SEUS. This is briefly examined by Goldstein et al. (2009), who find that the AOD and relative humidity (RH) at a single AERONET site (Walker Branch) are only weakly correlated across seasons. We investigate this further at several locations to better represent the effect of RH on a broader region of the SEUS. In addition, given that water uptake is already included in the simulation of AOD, we explore whether there is any evidence of a bias in RH in the GEOS-5 meteorology which could degrade the model simulation of AOD.

Hourly surface RH values used in GEOS-Chem are highly correlated with observations from the IMPROVE and SEARCH network nephelometer sites ($R = 0.6$–0.83, across sites and seasons) with a mean bias of less than 5 %. Correlations are highest during the morning and afternoon hours and degrade during the nighttime and at coastal sites (where GEOS-Chem has a low RH bias). Figure 4a demonstrates that there is little seasonality in mean surface RH in the SEUS, and that the model reproduces both the magnitude and consistency of RH year-round. Monthly RH values averaged over all the sites vary less than 10 % throughout the year at the 13:30 satellite overpass and less than 20 % when all hours are used to construct monthly means.

In order to examine the impact of these modest seasonal differences in RH on AOD, we use the optical properties applied to aerosols in GEOS-Chem to convert these differences in RH to differences in aerosol mass extinction efficiency. For simplicity, we use sulfate aerosol properties, which have the highest hygroscopicity (other than NaCl which is not a significant contributor to aerosol mass in the region) (Petters and Kreidenweis, 2007), and would be the most affected by changes in RH. At the surface,

CC BY

seasonal differences in mass extinction efficiency due to water uptake account for less than a 25 % increase in aerosol extinction from winter to summer over the SEUS (Fig. 4b).

The seasonality in the vertical profile of RH measured at the 8 NOAA sounding sites in the region is larger, with about a 20 % absolute increase in mean RH from winter to summer throughout the troposphere (Fig. 4c). However, seasonal difference in aerosol extinction resulting from water uptake (40 % when integrated over the column assuming sulfate aerosol) can account for only a fraction of the 100–300 % difference in AOD observed by the satellite instruments over the SEUS (Fig. 1). While this increase in summertime RH is generally captured by the model (and thus reflected in the simulated AOD seasonality), RH values in the lower troposphere (900–700 hPa) are slightly underestimated in summertime (<5 %). This translates to a 5–12 % underestimate in sulfate extinction efficiency in GEOS-Chem at these altitudes; however the effect is likely to be more modest for the mix of ambient aerosol with lower hygroscopicity. Therefore, aerosol water uptake cannot explain the observed seasonality in AOD, nor can biases in RH explain the model underestimate of this seasonality.

3.3 The vertical profile of aerosol

The lack of strong seasonality in surface aerosol concentrations and aerosol water content throughout the vertical column suggests that summertime increases in AOD over the SEUS must be associated with an increase in aerosol mass above the surface that is not accounted for in GEOS-Chem, potentially consistent with the hypothesis of Goldstein et al. (2009) which suggests a missing source of aerosols aloft.

Winter and summer vertical distributions of all the nighttime aerosol extinction values reported by CALIOP for three years (2007–2009) over the SEUS are shown in Fig. 5. The aerosol type is determined by an algorithm which considers the depolarization ratio, surface type, integrated backscatter, altitude and color ratio (Omar et al., 2009). Separating profiles based on aerosol type indicates broadly what sources are likely to contribute to the mass loading in each season, although the CALIOP algorithm is based on physical properties and does not distinguish aerosol by chemical composition.

Figure 5 shows that there are larger aerosol extinction observations at higher altitudes during the summer months. There is little seasonal difference in GEOS-5 nighttime boundary layer height (coincident with CALIOP measurements); but the deeper daytime mixed layers in summer may vertically distribute aerosol to higher altitudes. We investigate the impact of the mixing heights on the vertical profile in the next section.

In the final panels of Fig. 5, we compare the average nighttime profiles of aerosol extinction observed over the region by CALIOP with the average profile simulated by GEOS-Chem. First, these profiles confirm that the mean observed extinction profile over the SEUS is higher in the summer than in winter. The integrated mean AOD from these profiles increases more than 3-fold from winter to summer (0.07 to 0.25), consistent with the picture presented in Fig. 1. Second, these profiles demonstrate that the model underestimate of summertime AOD shown in Fig. 1 is associated with above-surface aerosols. Surface extinction values are reproduced by the model throughout the year, consistent with our $PM_{2.5}$ surface comparisons in Figs. 1 and 3. And while the simulated and observed profile shapes are similar in the wintertime, the model greatly under predicts aerosol extinction above the surface in summer. While there might be a biased in the CALIOP measurements near the surface (interference of clouds or lower sensitivity), the retrieval sensitivity of CALIOP increases with altitude (Winker et al., 2009), and Sheridan et al. (2012) suggest that if there is a bias in the free troposphere, it is a low bias, which suggest that the discrepancy in extinction above the surface between the simulated and measured profile is not due to CALIOP.

Mean summertime AOD calculated by integrating the model profile in Fig. 5 is 0.12, less than twice the mean CALIOP values. While these profiles do not suggest that there is a distinct lofted layer of aerosol, they do indicate that the seasonality in AOD is primarily associated with an increase in aerosol mass above the surface, in the lower troposphere (below 700 hPa), which is not captured by the GEOS-Chem model. This

CC BY

discrepancy is inconsistent with Heald et al. (2011) who show that the GEOS-Chem model generally captures the profiles of sulfate and organic aerosol in the Northern Hemisphere, even when concentrations are significantly underestimated.

We distinguish these CALIOP profiles by the observed aerosol types to understand the source of these aerosols, and Fig. 5 shows that the majority of aerosols observed in the SEUS are classified as polluted dust, polluted continental, and smoke. The maximum in dust above the boundary layer in the winter is likely due to dust transport from the western US while increases in the summer are associated with transport of African dust.

The summertime enhancement of extinction above the surface is predominantly associated with smoke and polluted continental aerosol types. This could indicate that aerosols from biomass burning are the cause of the seasonal difference. While previous studies have shown that biomass burning in the SEUS generally peaks in late winter and early spring (Zeng et al., 2008; Tian et al., 2009; Zhang et al., 2010), MODIS fire counts in this region almost double from winter to summer in 2007–2009. Furthermore, the GFED2 biomass burning emissions used in the model prescribe a factor of 3–4 increase from winter to summer for these years. However, this is largely offset by a decrease in emissions of carbonaceous aerosols from anthropogenic sources in summertime, such that increases in total emissions of carbonaceous aerosols are modest (20–30 %). This is consistent with the seasonal changes reported in simulated surface carbonaceous $PM_{2.5}$ (Fig. 3). Near the surface, smoke aerosols appear to have little impact; however, this is likely be due to the CALIOP algorithm, which generally requires that aerosols be in an elevated layer in order to be classified as smoke (Omar et al., 2009) and will otherwise be classified as polluted continental. Thus, aerosol identified by CALIOP as either polluted continental or smoke may be of the same chemical composition and origin and may not be directly linked to fire activity.

CC BY

3.4 Effect of planetary boundary layer height

One possible explanation of a large seasonal enhancement in AOD with modest change to surface $PM_{2.5}$ is a summertime aerosol source with a coincident deepening of the mixed layer. As shown in Fig. 5, this deepening of the daytime planetary boundary layer (PBL) is simulated in the GEOS-Chem model, with an increase of more than 60 hPa from winter to summer on average. The CALIOP average summer profile suggests that the higher concentrations above the surface are relatively uniform over a deep layer (up to 800 hPa), which could indicate that the GEOS-Chem simulation does not mix pollutants through a deep enough layer of the atmosphere, although we note that this altitude is similar to the mean summertime PBL depths used in the model (shown in Fig. 5). If the PBL heights used in the model are too shallow, pollutants could be trapped and more easily removed before being mixed upward.

The diurnal cycle of surface concentrations can provide some information about vertical mixing. For relatively constant emissions, surface concentrations generally increase at night with a shallow boundary layer and then as the PBL height grows throughout the day, pollutants are diluted and surface concentrations decline. Thus, a shallow bias in summertime afternoon mixed layer would reduce the diurnal variability in simulated $PM_{2.5}$ concentrations. However, the diurnal cycle of simulated and observed $PM_{2.5}$ at SEARCH sites are relatively similar (Fig. 2), with observations showing slightly more consistency throughout the day, especially in the summer months. The observations shown here are consistent with Weber et al. (2003) who show that on average $PM_{2.5}$ concentrations in Atlanta during August generally vary less than 20 % through the day due to sulfate peaking in the afternoon while OM, EC, and nitrate tend to peak in the early morning. Thus, while the contribution of the timing of different sources and mixing depths to the diurnal profile can be a challenge to untangle, the ability of the model to capture a relatively flat profile in surface $PM_{2.5}$, as well as the overall seasonality and composition of that $PM_{2.5}$ (Fig. 3), provides evidence of a relatively unbiased simulation of mixing depth.

cc BY

It remains a challenge to validate the PBL heights used in the model simulation as there are several different approaches used to estimate the height of the PBL, all of which can produce differing results (e.g. Berman et al., 1997). As shown in Marsik et al. (1995), various measurement systems can at some times differ on the height of the PBL over Atlanta by almost 1km. Therefore, we examine the sensitivity of the vertical profile and summertime AOD to changes in mixing depth. We performed four simulations for summer 2009, in which (1) PBL heights are raised by 100 hPa at all hours of the day, (2) PBL heights are raised by 100 hPa only during the daytime hours of 07:00 a.m. and 07:00 p.m. LST, (3) SO_2 emissions in North America are doubled, and (4) SO_2 emissions are doubled and the daytime PBL heights were raised. The impact of these simulations on the average regional profile is shown in Fig. 6.

Raising the PBL for all hours of the day increases extinction values throughout most of the profile, particularly at the top of the PBL, as concentrations are mixed throughout a deeper layer. However, values near the surface decrease as aerosols are mixed away from the surface into the deeper PBL, particularly at night. In the simulation where the PBL was only raised during the day, aerosol extinction values near the surface are similar to the original profile, but greater above the nighttime PBL, in the daytime residual layer. However, both of these simulations continue to substantially under predict the extinction values compared to CALIOP (AOD increases by only 0.02 over the region), suggesting that a potential bias in the PBL height would not be enough to explain the discrepancy in AOD.

Finally, we verify whether the aerosol profile measured by CALIOP is consistent with an increase in existing sources. We test increasing the sources of sulfate, which would be consistent with both the surface underestimate shown in Fig. 3, as well as the possibility of formation aloft via in-cloud processing. The profiles in Figure 6 demonstrate that doubling SO_2 emissions effectively scales up the entire simulated profile, but in doing so, significantly degrades the comparison at the surface. Simultaneously increasing the daytime PBL heights produces virtually the same profile, but produces an overestimate of observed aerosol extinction from 700 to 800 hPa. We therefore conclude that

cc BY

an increase in mixing depth, with or without a coincident increase in an existing aerosol source, cannot explain the observed CALIOP profile. This implies that the underestimate in aerosol mass aloft is due to an additional above-surface source.

4 Discussion

Satellite observations show a strong summertime enhancement in AOD over the SEUS, previously linked with biogenic activity, which is not observed in surface $PM_{2.5}$ concentrations. By determining here that there is little agreement between surface concentrations and column AOD in the Southeastern US , we then surmise that changes in surface mass concentrations do not control the seasonality of AOD in the region. Furthermore, the GEOS-Chem model generally captures observed surface concentrations (with the exception of a modest underestimate of summertime sulfate, and year-round underestimate of OA), but it does not reproduce the observed AOD seasonality, indicating an underestimation of aerosol extinction above the surface in the model. We show that neither a bias in model RH (and hence aerosol water uptake) nor summertime mixing depths can explain this discrepancy. Zhang et al. (2012b) show that GEOS-Chem reproduces wet deposition measurements in the US. This suggests that this discrepancy is also not due to a bias in aerosol removal, but rather a missing source of aerosol above the surface.

CALIOP measurements provide additional evidence of aerosol production above the surface; however, our interpretation is limited by the lack of aerosol chemical speciation. Ervens et al. (2011) suggest that in regions where there are large biogenic VOC and anthropogenic emissions, high RH, and cloudiness, yields from aqueous formation of SOA can be significant. Cloudy conditions, as well as enhanced oxidant concentrations in summertime, could also augment sulfate production, which we show is moderately underestimated in summertime in our simulation. GEOS-5 meteorology does show higher cloud fractions over the SEUS in the summer compared to the winter, which is corroborated by observations from MODIS Aqua and Terra (Fig. 7). If clouds are indeed serving as a medium for chemical production, this could explain the increased aerosol loading above the surface that is seen in the cloud-free CALIOP profiles shown here. However, observations from the CloudSat Cloud Profiling Radar suggest that mid to low troposphere cloud cover is highest in the region in winter (Fig. 7). Furthermore, we see no evidence of a correlation in daily cloud optical depth and aerosol extinction reported by CloudSat and CALIOP over the region. These conflicting characterizations of cloud seasonality, and a lack of correspondence between cloud cover and aerosol loading, suggest that cloud liquid water may not be the limiting factor in summertime aerosol production, but rather that the oxidation of biogenic VOCs whose emission peaks in summertime, is required to explain the observed aerosol enhancement above the surface.

It is vital, therefore, to have in situ vertical measurements of aerosol composition in order to fully investigate this hypothesis of increased aqueous aerosol production aloft and determine whether it is organic or inorganic in nature. The upcoming SOAS campaign aircraft data will be critical for resolving this issue and determining the aerosol characteristics in the SEUS, thus enabling a better prediction of how aerosol in this region is likely to evolve.

Acknowledgements. This work was supported by the National Science Foundation (ATM-0929282). We thank the satellite (MODIS, MISR, CALIOP, CloudSat) and in situ measurement teams (AERONET, IMPROVE, SEARCH).

References

Alexander, B., Park, R. J., Jacob, D. J., Li, Q. B., Yantosca, R. M., Savarino, J., Lee, C. C. W., and Thiemens, M. H.: Sulfate formation in sea-salt aerosols: Constraints from oxygen isotopes, J. Geophys. Res., 110, doi:10.1029/2004JD005659, D10307, 2005.

Al-Saadi, J., Szykman, J., Pierce, R. B., Kittaka, C., Neil, D., Chu, D. A., Remer, L., Gumley, L., Prins, E., Weinstock, L., MacDonald, C., Wayland, R., Dimmick, F., and Fishman, J.: Improving National Air Quality Forecasts with Satellite Aerosol Observations, B. Am. Meteorol. Soc., 86, 1249–1261, 2005.

cc BY

Alston, E. J., Sokolik, I. N., and Kalashnikova, O. V.: Characterization of atmospheric aerosol in the US Southeast from ground- and space-based measurements over the past decade, Atmos. Meas. Tech., 5, 1667–1682, doi:10.5194/amt-5-1667-2012, 2012.

Berman, S., Ku, J.-Y., Zhang, J., and Rao, S. T.: Uncertainties in estimating the mixing depth-comparing three mixing-depth models with profiler measurements, Atmos. Environ., 31, 3023–3039, 1997.

Blanchard, C. L., Hidy, G. M., Tanenbaum, S., and Edgerton, E. S.: NMOC, ozone, and organic aerosol in the southeastern United States, 1999–2007: 3. Origins of organic aerosol in Atlanta, Georgia, and surrounding areas, Atmos. Environ., 45, 1291–1302, 2011.

Chen, Y., Zheng, M., Edgerton, E. S., Ke, L., Sheng, G. and Fu, J.: PM2.5 source apportionment in the southeastern US : Spatial and seasonal variations during 2001–2005, J. Geophys. Res., 117, doi:10.1029/2011JD016572, D08304, 2012.

Chin, M., Savoie, D. L., Huebert, B. J., Bandy, A. R., Thornton, D. C., Bates, T. S., Quinn, P. K., Saltzman, E. S., and De Bruyn, W. J.: Atmospheric sulfur cycle simulated in the global model GOCART: Comparison with field observations and regional budgets, J. Geophys. Res., 105, 24689–24712, 2000.

Cooke, W. F., Liousse, C., Cachier, H. and Feichter, J.: Construction of a 1° ×1° fossil fuel emission data set for carbonaceous aerosol and implementation and radiative impact in the ECHAM4 model, J. Geophys. Res., 104, 22137–22,162, 1999.

Drury, E., Jacob, D. J., Spurr, R. J. D., Wang, J., Shinozuka, Y., Anderson, B. E., Clarke, A. D., Dibb, J., McNaughton, C. and Weber, R.: Synthesis of satellite (MODIS), aircraft (ICARTT), and surface (IMPROVE, EPA-AQS, AERONET) aerosol observations over eastern North America to improve MODIS aerosol retrievals and constrain surface aerosol concentrations and sources, J. Geophys. Res., 115, doi:10.1029/2009JD012629, D14204, 2010.

Duncan, B. N., Martin, R. V., Staudt, A. C., Yevich, R. and Logan, J. A.: Interannual and seasonal variability of biomass burning emissions constrained by satellite observations, J. Geophys. Res., 108, 4100, doi:10.1029/2002JD002378, 2003.

Edgerton, E. S., Hartsell, B. E., Saylor, R. D., Jansen, J. J., Hansen, D. A. and Hidy, G. M.: The Southeastern Aerosol Research and Characterization Study: Part II. Filter-based measurements of fine and coarse particulate matter mass and composition, J. Air Waste Manag Assoc., 55, 1527–1542, 2005.

Edgerton, E. S., Hartsell, B. E., Saylor, R. D., Jansen, J. J., Hansen, D. A. and Hidy, G. M.: The Southeastern Aerosol Research and Characterization Study, part 3: continuous

cc BY

measurements of fine particulate matter mass and composition, J. Air Waste. Manag. Assoc., 56, 1325–1341, 2006.

El-Zanan, H. S., Lowenthal, D. H., Zielinska, B., Chow, J. C. and Kumar, N.: Determination of the organic aerosol mass to organic carbon ratio in IMPROVE samples, Chemosphere, 60, 485–496, 2005.

Engel-Cox, J. A., Hoff, R. M., Rogers, R., Dimmick, F., Rush, A. C., Szykman, J. J., Al-Saadi, J., Chu, D. A. and Zell, E. R.: Integrating lidar and satellite optical depth with ambient monitoring for 3-dimensional particulate characterization, Atmos. Environ., 40, 8056–8067, 2006.

Ervens, B., Turpin, B. J., and Weber, R. J.: Secondary organic aerosol formation in cloud droplets and aqueous particles (aqSOA): a review of laboratory, field and model studies, Atmos. Chem. Phys., 11, 11069–11102, doi:10.5194/acp-11-11069-2011, 2011.

Fairlie, D. T., Jacob, D. J., and Park, R. J.: The impact of transpacific transport of mineral dust in the United States, Atmos. Environ., 41, 1251–1266, 2007.

Ford, B. and Heald, C. L.: An A-train and model perspective on the vertical distribution of aerosols and CO in the Northern Hemisphere, J. Geophys. Res., 117, doi:10.1029/2011JD016977, D06211, 2012.

Goldstein, A. H., Koven, C. D., Heald, C. L. and Fung, I. Y.: Biogenic carbon and anthropogenic pollutants combine to form a cooling haze over the southeastern United States, PNAS, 106, 8835–8840, 2009.

Guenther, A., Karl, T., Harley, P., Wiedinmyer, C., Palmer, P. I., and Geron, C.: Estimates of global terrestrial isoprene emissions using MEGAN (Model of Emissions of Gases and Aerosols from Nature), Atmos. Chem. Phys., 6, 3181–3210, doi:10.5194/acp-6-3181-2006, 2006.

Hallquist, Å. M., Jerksjö, M., Fallgren, H., Westerlund, J., and Sjödin, Å.: Particle and gaseous emissions from individual diesel and CNG buses, Atmos. Chem. Phys. Discuss., 12, 27737–27773, doi:10.5194/acpd-12-27737-2012, 2012.

Hand, J. L., Schichtel, B. A., Pitchford, M., Malm, W. C., and Frank, N. H.: Seasonal composition of remote and urban fine particulate matter in the United States, J. Geophys. Res., 117, doi:10.1029/2011JD017122, D05209, 2012.

Hansen, D. A., Edgerton, E. S., Hartsell, B. E., Jansen, J. J., Kandasamy, N., Hidy, G. M., and Blanchard, C. L.: The Southeastern Aerosol Research and Characterization Study: part 1 – Overview, J. Air Waste Manag. Assoc., 53, 1460–1471, 2003.

cc BY

Heald, C. L., Wilkinson, M. J., Monson, R. K., Alo, C. A., Wang, G., and Guenther, A.: Response of isoprene emission to ambient CO_2 changes and implications for global budgets, Glob. Change Biol., 15, 1127–1140, 2009.

Heald, C. L., Coe, H., Jimenez, J. L., Weber, R. J., Bahreini, R., Middlebrook, A. M., Russell, L. M., Jolleys, M., Fu, T.-M., Allan, J. D., Bower, K. N., Capes, G., Crosier, J., Morgan, W. T., Robinson, N. H., Williams, P. I., Cubison, M. J., DeCarlo, P. F., and Dunlea, E. J.: Exploring the vertical profile of atmospheric organic aerosol: comparing 17 aircraft field campaigns with a global model, Atmos. Chem. Phys., 11, 12673–12696, doi:10.5194/acp-11-12673-2011, 2011.

Heald, C. L., J. L. Collett Jr., Lee, T., Benedict, K. B., Schwandner, F. M., Li, Y., Clarisse, L., Hurtmans, D. R., Van Damme, M., Clerbaux, C., Coheur, P.-F., Philip, S., Martin, R. V., and Pye, H. O. T.: Atmospheric ammonia and particulate inorganic nitrogen over the United States, Atmos. Chem. Phys., 12, 10295–10312, doi:10.5194/acp-12-10295-2012, 2012.

Henze, D. K., Seinfeld, J. H., Ng, N. L., Kroll, J. H., Fu, T.-M., Jacob, D. J., and Heald, C. L.: Global modeling of secondary organic aerosol formation from aromatic hydrocarbons: high- vs. low-yield pathways, Atmos. Chem. Phys., 8, 2405–2420, doi:10.5194/acp-8-2405-2008, 2008.

Holben, B. N., Eck, T. F., Slutsker, I., Tanré, D., Buis, J. P., Setzer, A., Vermote, E., Reagan, J. A., Kaufman, Y. J., Nakajima, T., Lavenu, F., et al.: AERONET—A Federated Instrument Network and Data Archive for Aerosol Characterization, Remote Sens. Environ., 66, 1–16, 1998.

Hoyle, C. R., Boy, M., Donahue, N. M., Fry, J. L., Glasius, M., Guenther, A., Hallar, A. G., Huff Hartz, K., Petters, M. D., Petäjä, T., Rosenoern, T., and Sullivan, A. P.: A review of the anthropogenic influence on biogenic secondary organic aerosol, Atmos. Chem. Phys., 11, 321–343, doi:10.5194/acp-11-321-2011, 2011.

Hudman, R. C., Jacob, D. J., Turquety, S., Leibensperger, E. M., Murray, L. T., Wu, S., Gilliland, A. B., Avery, M., Bertram, T. H., Brune, W., Cohen, R. C., Dibb, J. E., Flocke, F. M., Fried, A., Holloway, J., Neuman, J. A., Orville, R., Perring, A., Ren, X., Sachse, G. W., Singh, H. B., Swanson, A., and Wooldridge, P. J.: Surface and lightning sources of nitrogen oxides over the United States: Magnitudes, chemical evolution, and outflow, J. Geophys. Res., 112, doi:10.1029/2006JD007912, D12S05, 2007.

Hudman, R. C., Murray, L. T., Jacob, D. J., Millet, D. B., Turquety, S., Wu, S., Blake, D. R., Goldstein, A. H., Holloway, J., and Sachse, G. W.: Biogenic versus anthropogenic sources

cc BY

of CO in the United States, Geophys. Res. Lett., 35, doi:10.1029/2007GL032393, L04801, 2008.

Hunt, W. H., Winker, D. M., Vaughan, M. A., Powell, K. A., Lucker, P. L., and Weimer, C.: CALIPSO Lidar Description and Performance Assessment, J. Atmos. Ocean. Tech., 26, 1214–1228, 2009.

Jaeglé, L., Quinn, P. K., Bates, T. S., Alexander, B., and Lin, J.-T.: Global distribution of sea salt aerosols: new constraints from in situ and remote sensing observations, Atmos. Chem. Phys., 11, 3137–3157, 2011, http://www.atmos-chem-phys.net/11/3137/2011/.

Koepke, P., Hess, M., Schult, I., and Shettle, E. P.: Global Aerosol Data Set, Max-Planck-Institut für Meteorologie, Hamburg, Germany, 1997.

Leibensperger, E. M., Mickley, L. J., Jacob, D. J., Chen, W.-T., Seinfeld, J. H., Nenes, A., Adams, P. J., Streets, D. G., Kumar, N., and Rind, D.: Climatic effects of 1950–2050 changes in US anthropogenic aerosols – Part 1: Aerosol trends and radiative forcing, Atmos. Chem. Phys., 12, 3333–3348, doi:10.5194/acp-12-3333-2012, 2012.

Lim, H.-J. and Turpin, B. J.: Origins of Primary and Secondary Organic Aerosol in Atlanta: Results of Time-Resolved Measurements during the Atlanta Supersite Experiment, Environ. Sci. Technol., 36, 4489–4496, 2002.

Liu, H., Jacob, D. J., Bey, I., and Yantosca, R. M.: Constraints from 210Pb and 7Be on wet deposition and transport in a global three-dimensional chemical tracer model driven by assimilated meteorological fields, J. Geophys. Res., 106, 12109–12128, 2001.

Malm, W. C. and Hand, J. L.: An examination of the physical and optical properties of aerosols collected in the IMPROVE program, Atmos. Environ., 41, 3407–3427, 2007.

Malm, W. C., Sisler, J. F., Huffman, D., Eldred, R. A. and Cahill, T. A.: Spatial and seasonal trends in particle concentration and optical extinction in the United States, J. Geophys. Res., 99, 1347–1370, 1994.

Marsik, F. J., Fischer, K. W., McDonald, T. D., and Samson, P. J.: Comparison of Methods for Estimating Mixing Height Used during the 1992 Atlanta Field Intensive, J. Appl. Meteorol., 34, 1802–1814, 1995.

Martin, R. V., Jacob, D. J., Yantosca, R. M., Chin, M., and Ginoux, P.: Global and regional decreases in tropospheric oxidants from photochemical effects of aerosols, J. Geophys. Res., 108, 4097, doi:10.1029/2002JD002622, 2003.

Omar, A. H., Winker, D. M., Vaughan, M. A., Hu, Y., Trepte, C. R., Ferrare, R. A., Lee, K.-P., Hostetler, C. A., Kittaka, C., Rogers, R. R., Kuehn, R. E., and Liu, Z.: The CALIPSO Automated Aerosol Classification and Lidar Ratio Selection Algorithm, J. Atmos. Ocean. Tech., 26, 1994–2014, 2009.

Park, R. J., Jacob, D. J., Chin, M., and Martin, R. V.: Sources of carbonaceous aerosols over the United States and implications for natural visibility, J. Geophys. Res., 108, 2002–3190, 2003.

Park, R. J., Jacob, D. J., Field, B. D., Yantosca, R. M. and Chin, M.: Natural and transboundary pollution influences on sulfate-nitrate-ammonium aerosols in the United States: Implications for policy, J. Geophys. Res., 109, D15204, doi:10.1029/2003JD004473, 2004.

Peltier, R. E., Sullivan, A. P., Weber, R. J., Wollny, A. G., Holloway, J. S., Brock, C. A., de Gouw, J. A. and Atlas, E. L.: No evidence for acid-catalyzed secondary organic aerosol formation in power plant plumes over metropolitan Atlanta, Georgia, Geophys. Res. Lett., 34, doi:10.1029/2006GL028780, L06801, 2007.

Petters, M. D. and Kreidenweis, S. M.: A single parameter representation of hygroscopic growth and cloud condensation nucleus activity, Atmos. Chem. Phys., 7, 1961–1971, doi:10.5194/acp-7-1961-2007, 2007.

Portmann, R. W., Solomon, S., and Hegerl, G. C.: Spatial and seasonal patterns in climate change, temperatures, and precipitation across the United States, PNAS, 106(18), 7324–7329, 2009.

Remer, L. A., Tanré, D., Kaufman, Y. J., Ichoku, C., Mattoo, S., Levy, R., Chu, D. A., Holben, B., Dubovik, O., Smirnov, A., Martins, J. V., Li, R.-R., and Ahmad, Z.: Validation of MODIS aerosol retrieval over ocean, Geophys. Res. Lett., 29, 8008, doi:10.1029/2001GL013204, 2002.

Ridley, D. A., Heald, C. L., and Ford, B.: North African dust export and deposition: A satellite and model perspective, J. Geophys. Res., 117, D02202, doi:10.1029/2011JD016794, 2012.

Roy, B., Mathur, R., Gilliland, A. B., and Howard, S. C.: A comparison of CMAQ-based aerosol properties with IMPROVE, MODIS, and AERONET data, J. Geophys. Res., 112, doi:10.1029/2006JD008085, D14301, 2007.

Stephens, G. L., Vane, D. G., Boain, R. J., Mace, G. G., Sassen, K., Wang, Z., Illingworth, A. J., O'Connor, E. J., Rossow, W. B., Durden, S. L., Miller, S. D., Austin, R. T., Benedetti, A., Mitrescu, C., and Cloudsat Science Team: The CLOUDSAT Mission and the A-Train, B. Am. Meteorol. Soc., 83, 1771–1790, 2002.

CC BY

Stephens, G. L., Vane, D. G., Tanelli, S., Im, E., Durden, S., Rokey, M., Reinke, D., Partain, P., Mace, G. G., Austin, R., L'Ecuyer, T., Haynes, J., Lebsock, M., Suzuki, K., Waliser, D., Wu, D., Kay, J., Gettelman, A., Wang, Z., and Marchand, R.: CloudSat mission: Performance and early science after the first year of operation, J. Geophys. Res., 113, D00A18, doi:10.1029/2008JD009982, 2008.

Tegen, I. and Lacis, A. A.: Modeling of particle size distribution and its influence on the radiative properties of mineral dust aerosol, J. Geophys. Res., 101, 19237–19244, 1996.

Tian, D., Hu, Y., Wang, Y., Boylan, J. W., Zheng, M., and Russell, A. G.: Assessment of biomass burning emissions and their impacts on urban and regional PM2.5: a Georgia case study, Environ. Sci. Technol., 43, 299–305, 2009.

van der Werf, G. R., Randerson, J. T., Giglio, L., Collatz, G. J., Kasibhatla, P. S., and Arellano Jr., A. F.: Interannual variability in global biomass burning emissions from 1997 to 2004, Atmos. Chem. Phys., 6, 3423–3441, doi:10.5194/acp-6-3423-2006, 2006.

van Donkelaar, A., Martin, R. V., and Park, R. J.: Estimating ground-level PM2.5 using aerosol optical depth determined from satellite remote sensing, J. Geophys. Res., 111, D21201, doi:10.1029/2005JD006996, 2006.

van Donkelaar, A., Martin, R. V., Brauer, M., Kahn, R., Levy, R., Verduzco, C., and Villeneuve, P. J.: Global estimates of ambient fine particulate matter concentrations from satellite-based aerosol optical depth: development and application, Environ. Health Perspect., 118, 847–855, doi:10.1289/ehp.0901623, 2010.

Volkamer, R., Jimenez, J. L., Martini, F. S., Dzepina, K., Zhang, Q., Salcedo, D., Molina, L. T., Worsnop, D. R., and Molina, M. J.: Secondary organic aerosol formation from anthropogenic air pollution: Rapid and higher than expected, Geophys. Res. Lett., 33, doi:10.1029/2006GL026899, L17811, 2006.

Wang, Y., Jacob, D. J., and Logan, J. A.: Global simulation of tropospheric O3-NO x -hydrocarbon chemistry 3. Origin of tropospheric ozone and effects of nonmethane hydrocarbons, J. Geophys. Res., 103, 10757–10,767, 1998.

Weber, R., Bergin, M., Kiang, C. S., Chameides, W., Orsini, D., St, J. J., Chang, M., Bergin, M., Carrico, C., Lee, Y. N., Dasqupta, P., Slanina, J., Turpin, B., Edgerton, E., Hering, S., Allen, G., and Solomon, P.: Short-term temporal variation in PM2.5 mass and chemical composition during the Atlanta Supersite Experiment, 1999, J. Air Waste Manag. Assoc., 53, 84–91, 2003.

Weber, R. J., Sullivan, A. P., Peltier, R. E., Russell, A., Yan, B., Zheng, M., Gouw, J. de, Warneke, C., Brock, C., Holloway, J. S., Atlas, E. L., and Edgerton, E.: A study of secondary organic aerosol formation in the anthropogenic-influenced southeastern United States, J. Geophys. Res., 112(D13), doi:10.1029/2007JD008408, D13302, 2007.

Wesely, M. L.: Parameterization of surface resistances to gaseous dry deposition in regional-scale numerical models, Atmos. Environ., 23, 1293–1304, 1989.

Winker, D. M.: The CALIPSO mission: spaceborne lidar for observation of aerosols and clouds, SPIE, 4893, 1–11, 2003.

Winker, D. M., Vaughan, M. A., Omar, A., Hu, Y., Powell, K. A., Liu, Z., Hunt, W. H., and Young, S. A.: Overview of the CALIPSO Mission and CALIOP Data Processing Algorithms, J. Atmos. Ocean. Tech., 26, 2310–2323, 2009.

Yan, B., Zheng, M., Hu, Y., Ding, X., Sullivan, A. P., Weber, R. J., Baek, J., Edgerton, E. S., and Russell, A. G.: Roadside, urban, and rural comparison of primary and secondary organic molecular markers in ambient PM2.5, Environ. Sci. Technol., 43, 4287–4293, 2009.

Zeng, T., Wang, Y., Yoshida, Y., Tian, D., Russell, A. G., and Barnard, W. R.: Impacts of prescribed fires on air quality over the Southeastern United States in spring based on modeling and ground/satellite measurements, Environ. Sci. Technol., 42, 8401–8406, 2008.

Zhang, H., Hoff, R. M., and Engel-Cox, J. A.: The relation between Moderate Resolution Imaging Spectroradiometer (MODIS) aerosol optical depth and PM2.5 over the United States: a geographical comparison by US Environmental Protection Agency regions, J. Air Waste Manag. Assoc., 59, 1358–1369, 2009.

Zhang, J. and Reid, J. S.: MODIS aerosol product analysis for data assimilation: Assessment of over-ocean level 2 aerosol optical thickness retrievals, J. Geophys. Res., 111, D22207, doi:10.1029/2005JD006898, 2006.

Zhang, L., Jacob, D. J., Knipping, E. M., Kumar, N., Munger, J. W., Carouge, C. C., van Donkelaar, A., Wang, Y. X., and Chen, D.: Nitrogen deposition to the United States: distribution, sources, and processes, Atmos. Chem. Phys., 12, 4539–4554, doi:10.5194/acp-12-4539-2012, 2012b.

Zhang, X., Hecobian, A., Zheng, M., Frank, N. H., and Weber, R. J.: Biomass burning impact on $PM_{2.5}$ over the southeastern US during 2007: integrating chemically speciated FRM filter measurements, MODIS fire counts and PMF analysis, Atmos. Chem. Phys., 10, 6839–6853, doi:10.5194/acp-10-6839-2010, 2010.

Zhang, X., Liu, Z., Hecobian, A., Zheng, M., Frank, N. H., Edgerton, E. S., and Weber, R. J.: Spatial and seasonal variations of fine particle water-soluble organic carbon (WSOC) over the southeastern United States: implications for secondary organic aerosol formation, Atmos. Chem. Phys., 12, 6593–6607, doi:10.5194/acp-12-6593-2012, 2012.

Zheng, M., Cass, G. R., Schauer, J. J., and Edgerton, E. S.: Source Apportionment of PM2.5 in the Southeastern United States Using Solvent-Extractable Organic Compounds as Tracers, Environ. Sci. Technol., 36, 2361–2371, 2002.

Table 1. Mass extinction efficiency values used in GEOS-Chem for sulfate aerosols at given relative humidity values.

Relative Humidity (%)	Mass Extinction Efficiency (m^2g^{-1})
0	2.24
50	6.12
70	8.90
80	11.90
90	19.09
95	32.75
99	104

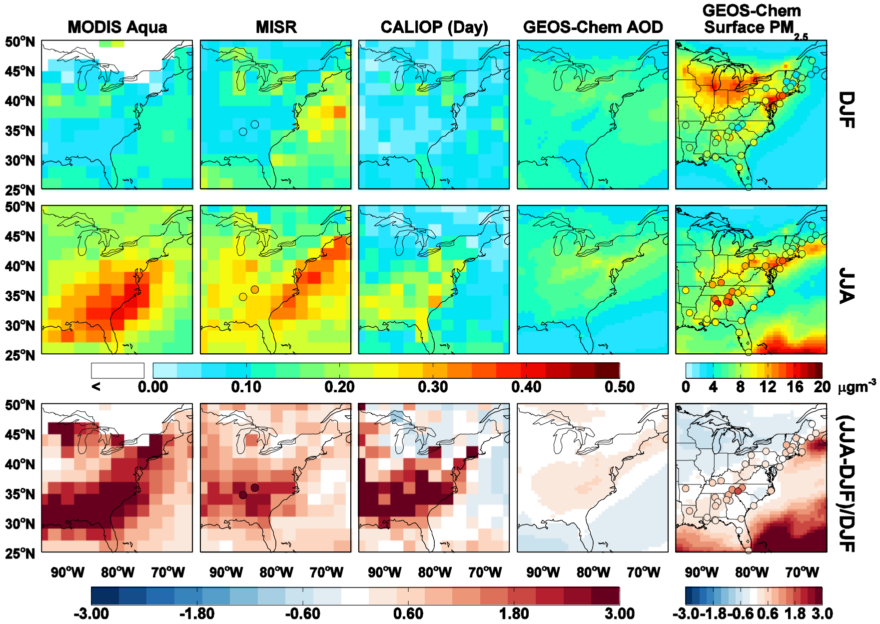

Fig. 1. Seasonally averaged total column AOD for winter (DJF, top row) and summer (JJA, middle row) for December 2006–August 2009 as observed by MODIS (column 1), MISR (column 2), and CALIOP (daytime, column 3) gridded to 2° × 2.5° and compared to simulated AOD from GEOS-Chem (column 4). Concentrations of surface $PM_{2.5}$ simulated by GEOS-Chem are overlaid with concentrations measured at IMPROVE and SEARCH network sites (circles) in column 5. Bottom row shows the relative enhancement of summer over winter for observed and simulated AOD and surface concentrations. Average AOD observed at the University of Alabama, Huntsville and Walker Branch AERONET sites for 2008–2009 is overlaid on the MISR maps.

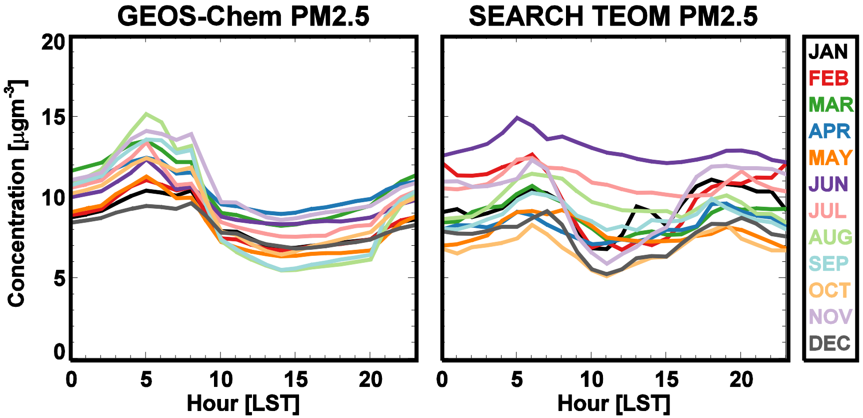

Fig. 2. Diurnal cycles of monthly mean $PM_{2.5}$ concentrations as simulated by GEOS-Chem **(a)** and as measured by TEOM filters at SEARCH network sites **(b)**, color coded by month in 2009 over which the averaging was done.

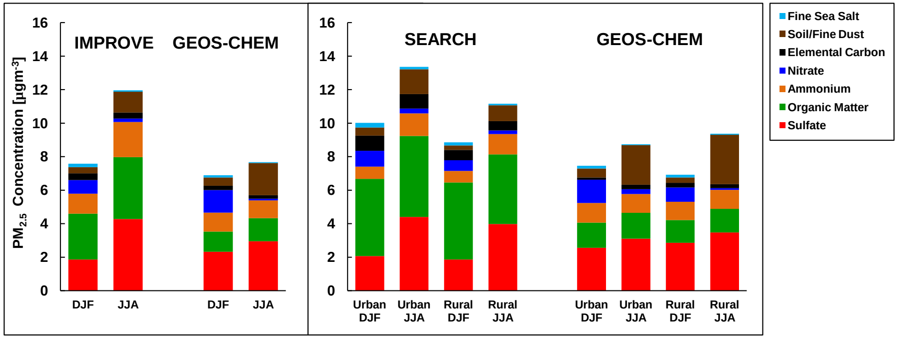

Fig. 3. Mean seasonally averaged surface mass concentrations of $PM_{2.5}$ **(a)** observed at the 13 IMPROVE network sites in the SEUS and as simulated by GEOS-Chem (sampled to the IMPROVE sampling days and corresponding model grid boxes). **(b)** Same as **(a)** for SEARCH network sites. All data is for December 2006–2009, except for SEARCH sea salt, which only uses data from 2009.

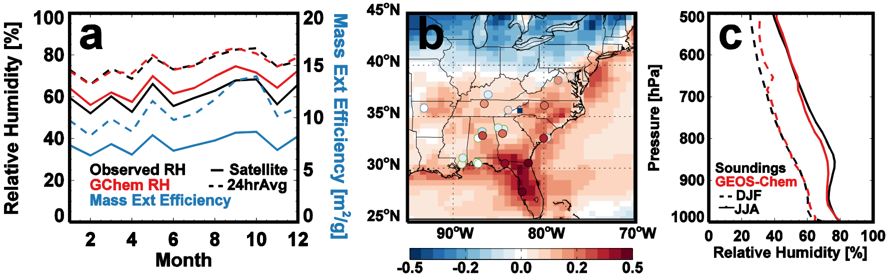

Fig. 4. (a) Average 2009 monthly surface RH recorded at IMPROVE and SEARCH network nephelometer sites (black) using 24 h averages (dashed line) and sampled to the afternoon overpass time (solid line). These are compared with values used in GEOS-Chem (red lines) sampled to observational site locations and converted to mass extinction efficiency values (for sulfate aerosols, blue lines). **(b)** Fractional increase in surface mass extinction efficiency of summer over winter simulated with GEOS-Chem and overlaid with values calculated from surface RH observed at IMPROVE nephelometer (blue circles), SEARCH (green circles) and sounding (black circles) sites for 2009. GEOS-Chem, SEARCH and IMPROVE data are sampled for the afternoon satellite overpass time (13:00–15:00 LT) and the sounding data is an average from 0000 and 1200 UTC. **(c)** mean profile of RH measured at the 8 sounding sites (black lines) at 00:00 and 12:00 UTC and the corresponding RH in GEOS-Chem (red line) sampled to the site locations and times for winter (dashed) and summer (solid) 2009.

Title Page
Abstract | Introduction
Conclusions | References
Tables | Figures
◄| |►
◄ ►
Back | Close
Full Screen / Esc
Printer-friendly Version
Interactive Discussion

ACPD
13, 9917–9952, 2013

Aerosol loading in the Southeastern United States

B. Ford and C. L. Heald

CC BY

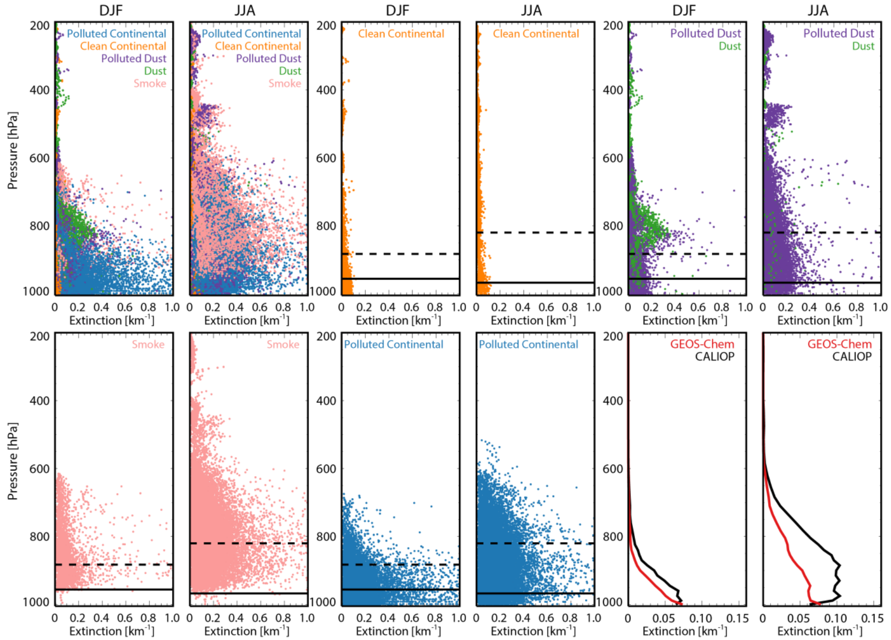

Fig. 5. All nighttime aerosol extinction values observed by CALIOP for winter and summer seasons of 2007–2009 over the SEUS (30.5° N to 37.5° N and 90° W to 81.5° W). Values are colored by classified aerosol types. There are ∼70 000 extinction values shown for the winter and ∼200 000 for the summer from 2006–2009, including values below the detection limit. Panels 1 and 2 show all values, and panels 3-10 separate values based on aerosol type with seasonally averaged boundary layer heights from GEOS-Chem for nighttime (solid black horizontal lines) and daytime (dashed lines) overlaid. Bottom right panels show average aerosol extinction profiles as observed by CALIOP (black) and the corresponding profiles simulated by GEOS-Chem and sampled to the CALIOP overpasses (red) for the two seasons applying detection limits as in Ford and Heald (2012).

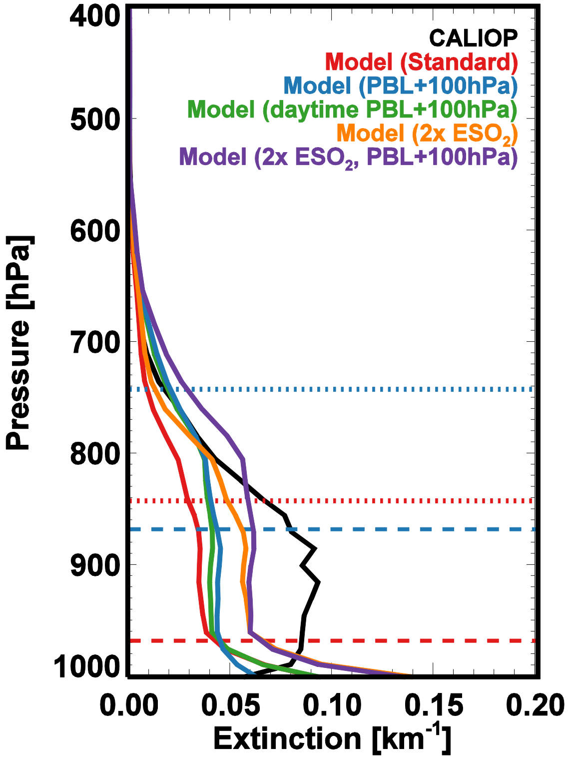

Fig. 6. Aerosol extinction profiles over the SEUS for JJA 2009 as observed by CALIOP (black) and as simulated by GEOS-Chem with original PBL heights (red), PBL heights raised by 100 hPa at all hours (blue), raised by 100 hPa during daytime hours (green), doubled SO_2 emissions (orange), and doubled SO_2 emissions and PBL heights raised during daytime hours (purple). Average PBL heights are shown in red for original simulation and blue for simulations with raised PBL heights, with dashed lines for nighttime and dotted lines for daytime.

cc BY

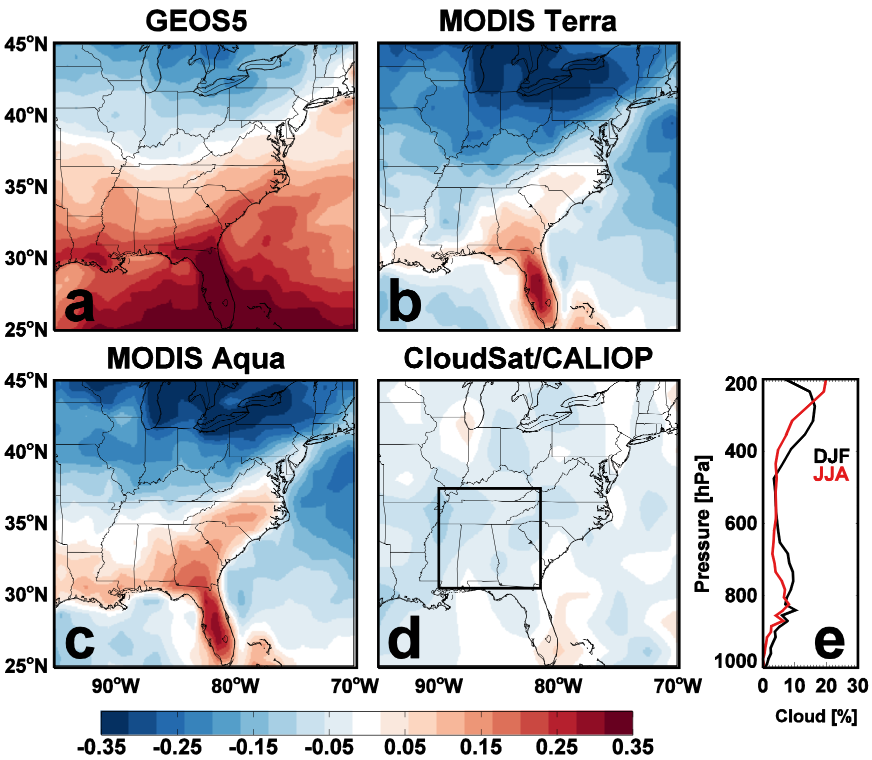

Fig. 7. Differences (summer-winter) between average cloud fraction for 2006–2009 from **(a)** GEOS-5 sampled to afternoon overpass, **(b)** observed by MODIS onboard Terra **(c)** Aqua, and **(d)** observed by CloudSat/CALIOP. Black outline shows region for profiles of average cloud fraction over the SEUS for winter (black) and summer (red) observed by CloudSat/CALIOP in 2009 shown in panel **(e)**.

Title Page
Abstract
Introduction
Conclusions
References
Tables
Figures
◀|
|▶
◀
▶
Back
Close
Full Screen / Esc
Printer-friendly Version
Interactive Discussion